A.G. Yessengaliyev [1] , A.B. Mukanov [2]

[1] *Ghalam LLP, Turan avenue, 89, Astana, Kazakhstan*
[2] *Kazakhstan Branch of Lomonosov Moscow State University, Kazhymukan str. 11, Astana, Kazakhstan*
(E-mail: arman.gibatovich@gmail.com, mukanov.askhat@gmail.com)

High-precision satellite orbit propagation with estimation of the covariance matrix [1]

Abstract: In this paper is proposed to use a model of high-precision propagation of the satellite position, in which the disturbing accelerations are determined, and the obtained numerical results are presented.

All disturbing forces acting on the satellite are modeled, the up-to-date data of the parameters of the atmospheric drag model, as well as the parameters IERS, EOP are used. The developed software for satellite orbit propagation is applicable to support the flight control of the satellite, while ensuring the accuracy of the level of 10-15 meters along the position vector of the satellite over a weekly time interval.

With a given model of satellite motion and known statistical characteristics of orbit determination errors, the covariance matrix is predicted along with the state vector, which has found application in many applied tasks for support of Flight dynamics activities.

Keywords: Satellite, Orbit Propagator, Orbit Determination, Low Earth Orbit, orbit estimation, perturbing forces, numerical integration, Runge-Kutta methods, Covariance Matrix.

2000 Mathematics Subject Classification: 65L05, 70F15

1. Introduction. The main purpose of this work is to build a model for high-precision propagation of the satellite position, taking into account the main disturbing accelerations acting on a satellite in low-Earth orbit (LEO). For Satellite missions with a Payload in LEO, a high accuracy of propagation the position in the satellite orbit is required to solve most of the tasks of ballistic and navigation support of the orbit control flight to fulfill the target mission of the satellite.

The state vector of the satellite can be represented as a six-dimensional vector consisting of a position vector and a velocity vector of the satellite, or as a more extended vector, including in addition the specified coefficient of reflectivity C_R and atmospheric drag coefficient C_D.

For a satellite mission in LEO, the maximum value of the norm of the discrepancy vector between the propagated and the true (reference) vector of the satellite state over one week interval characterizes the accuracy of propagation the position in the satellite orbit. Under the high-precision propagation of the position in the orbit of the satellite, the value of 100 m is assumed along the position vector and along the velocity vector of 0.02 m/s.

Methods of propagation the position of the satellite are widely known, which uses semi-analytical and analytical methods (for example, SGP4, Brower-Lydanne theory, PPT3), as well as more accurate ones using numerical methods.

There are many products on the world market that solve similar problems in propagation the orbit of a satellite. An overview of large products, which include a module for propagation the position of the satellite in orbit using numerical integration of the equations of motion, is presented in Table 1.

TABLE 1 – Software that includes a module for satellite orbit propagation

Organization	Software	Integration model or method
Analytical Graphics Inc.	STK	Runga Kutta, Gauss-Jackson
NASA/JPL(1990)	GIPSY/OASIS II Real-Time GIPSY	High-order Adams predictor-corrector
NASA/GSFC(1975)	GTDS	4th-order Runga Kutta, Cowell Adams predictor-corrector
NRL (1996)	OCEANS	Cowell 4th-order Runga Kutta, 9th order Predictor-corrector
TRACE	Aerospace Corp. (Air Force)	10th-order Gauss-Jackson w/ regularized time option
NASA and other	GMAT[1]	Runge-Kutta ,Runge-Kutta89, Runge-Kutta-Fehlberg56

Also among the large and developing products are the following:
FreeFlyer[2] (ai-solutions), Goddard Trajectory Determination System (GTDS), Java Astrodynamics Toolkit(JAT)[3], focusSuite (GMV)[4], Quartz(Airbus)[5], ORSA[6]. However, most of them represent commercial products with a high price, some with limited functionality, and an annual paid license is required for support. At the same time, most of the products distributed for free, built on simplified models, give errors of several hundred meters or more at an interval of 3 days or more.

The OPT software developed by us for high-precision propagation of the satellite orbit can be used for the mission of domestic remote sensing satellite for use in routine operation of the satellite, while reducing the need to purchase expensive foreign software. The developed OPT software has a number of functional features and advantages:

- Portability: The design and technology stack guarantees the portability of the product to various operating systems and simplifies the deployment of the product;
- Modularity and extensibility: The software is designed as modular and extensible;
- Adaptability: applicable for satellite missions in low Earth orbit, as well as for other types of orbits;
- High accuracy of propagation the position of the satellite in orbit;
- Multithreading;
- Rich graphical user interface.

Section 2 describes numerical integration methods and describes a dynamic model of disturbing forces. The main method that reduces the error of calculations is the method of numerical integration of differential equations describing the motion of the satellite. We consider the Runge-Kutta method with the Dormand-Prince modification (DOPRI 8(7)) [1]. In section

---

[1]General Mission Analysis Tool, Software Package, NASA Goddard Space Flight Center, Greenbelt, MD, 2007, URL: http://gmat.gsfc.nasa.gov

[2]FreeFlyer, a.i. solutions Inc. FreeFlyer. URL: https://ai-solutions.com/freeflyer/.

[3]Java Astrodynamics Toolkit

[4]focusSuite (GMV), https://www.gmv.com/en/products/space/focussuite

[5]Quartz(Airbus Defence and Space flight dynamics software), www.airbus.com

[6]Orbit Reconstruction, Simulation and Analysis. Pasquale Tricarico. ORSA. http://orsa.sourceforge.net/

Bulletin of L.N. Gumilyov ENU. Mathematics. Computer science. Mechanics series, 2022, Vol. 141, №4

7

3, a brief description of the software developed for high-precision propagation of the satellite position is given, the modeling input data with which calculations were performed, and the results of calculations are given. Section 4 provides conclusions based on the results of calculations.

2. Mathematical formulation of the problem

2.1. Dynamic model

The propagation of the satellite state vector in orbit is based on a dynamic model of forces, including the Earth's gravity, polar and ocean tides, lunar-solar disturbances, atmospheric drag and solar radiation pressure, as well as relativistic effects.

Some perturbed accelerations are represented using precise analytical (semi-analytical) formulas or using numerical methods.

A dynamic model for propagation satellite motion is described by a system of the second-order ODEs (Ordinary differential equations) that is solved numerically with the method of integrating the Runge-Kutta with the Dormand-Prince modification. In this case, the components of the velocity vector and the components of the acceleration vector of perturbing forces are contained on the right-hand side of the system of equations.

It is assumed that the vectors $\vec{r} = (x, y, z)$ и $\vec{v} = (v_x, \ v_y, v_z)$ determining the position and velocity of the satellite, are set in an Earth Centered Inertial coordinate system (ECI J2000 frame). The equations of motion of the satellite have the form:

$$\text{f}\,(\text{x},\text{t}) = \left(\begin{array}{c} \dot{\vec{r}} \\ \dot{\vec{v}} \end{array} \right) = \left(\begin{array}{c} v_x \\ v_y \\ v_z \\ a_x \\ a_y \\ a_z \end{array} \right) \tag{1}$$

$$\vec{a} = -\frac{\mu}{r^3}\vec{r} + \vec{a}_{Earth} + \vec{a}_{asp} + \vec{a}_{tide} + \vec{a}_{3Bodies} + \vec{a}_{drag} + \vec{a}_{PN_{eff}} + \vec{a}_{other}, \tag{2}$$

where $\vec{a} = \frac{d^2\vec{r}}{dt^2}$ – acceleration equal to the sum of all accelerations [2, p. 525] due to the action of disturbing forces on the satellite, and the terms from the right part describe disturbances caused by the gravitational field of the Earth, solid and ocean tides, disturbances of the Sun and Moon, solar radiation pressure, atmospheric drag effects, Post-Newtonian corrections. The remaining shortcomings of the force models are compensated by empirical accelerations, which are corrected together with other parameters on orbit determination process.

Earth Gravity Models. It is convenient to determine the potential of the Earth's gravitational field in a geocentric equatorial coordinate system rotating with the Earth. The potential of the Earth's gravitational field is expressed in the form of expansion by spherical harmonic functions in a geocentric Earth-fixed reference frame [3]:

$$U(r, \lambda, \varphi) = \frac{\mu}{r} \left(1 + \sum_{n=2}^{\infty} \sum_{m=0}^{n} \left(\frac{R_{\oplus}}{r} \right)^n (C_{n,m}\cos m\lambda + S_{n,m}\sin m\lambda\,) P_{n,m}(\sin \varphi\,) \right) \tag{3}$$

where μ – Gravitational Parameter of Earth; $\mu = G \cdot M\ = 398{,}6005{\cdot}1012$ м3/с2;
G –the universal gravitational constant of the Earth;
M – Earth mass;
r – the distance from the center of mass of the Earth to the point in space where the potential is calculated;
$R_{\oplus}$ – the average radius of the Earth;
φ, λ – geocentric coordinates of the satellite (latitude, longitude of a spacecraft mass point);
$C_{n,m}, S_{n,m}$ – the gravitational coefficients of sectorial harmonics at $n = m$ and tesseral harmonics at $n \neq m$;
$P_{n,m}(\sin \varphi\,)$ – the associated Legendre functions of degree n and order m, which are calculated by recurrence relations.

Л.Н. Гумилев атындағы ЕҰУ Хабаршысы. Математика. Компьютерлік ғылымдар. Механика, 2022, Том 141, №4
Вестник ЕНУ им. Л.Н. Гумилева. Математика. Компьютерные науки. Механика, 2022, Том 141, №4

8

Imagine U in the form: $U = U_0 + U_1$, where

$$U_0 = \frac{\mu}{r},$$

$$U_1 = \sum_{n=2}^{\infty} \sum_{m=0}^{n} u_{nm}$$

$$u_{nm} = \frac{\mu}{r} \left(\frac{R_\oplus}{r} \right)^n (C_{n,m} \cos m\lambda + S_{n,m} \sin m\lambda) P_{n,m} (\sin \varphi).$$

The components of acceleration due to a nonspherical central body are partial derivatives of the geopotential U in geocentric Cartesian coordinates x, y, z:

$$(\vec{a}_{Earth})'_x = -\mu \frac{x}{r^3} + \frac{\partial U_1}{\partial x},$$

$$(\vec{a}_{Earth})'_y = -\mu \frac{y}{r^3} + \frac{\partial U_1}{\partial y},$$

$$(\vec{a}_{Earth})'_z = -\mu \frac{z}{r^3} + \frac{\partial U_1}{\partial z},$$

To describe the Earth's gravitational field, we use the models $EarthGravityModel96(EGM96)$ and $EarthGravityModel2008(EGM2008)$ [4]. The software implements models of the earth's gravitational field $EGM96/EGM2008$ in the form of expansion in a series of spherical functions, providing accounting for the full number of harmonics up to 71 degrees inclusive with the possibility of selective accounting of harmonics. But it is possible to use the maximum degree and order of 2190x2190, but at the same time a significant decrease in performance (long computing time) does not pay off with a significant improvement in accuracy compared to non-simulated perturbations.

Rotations corresponding to Precession, Nutation and Pole movement of Earth's rotation axis are taken into account on coordinate transformations between Celestial to Terrestrial reference frames.

Solid and ocean tides. The tides of the Earth (solid and oceanic) are given by the k_{20}, model considered in [5].

Perturbations from tidal deformations of the central body make a noticeable contribution to the composition of perturbing accelerations.

The gravitational influence of the Sun, Moon and large planets causes deformations of the Earth, as a result of which its gravitational field changes. The simplest model for representing the potential of the forces acting on the satellite due to tidal deformations of the Earth is the Love model [6] or the model of solid tides. More accurate models take into account the influence of tidal deformations occurring in the ocean and in the Earth's atmosphere. Then the influence of tides can be modeled through corrections to the coefficients of the Earth's geopotential S_{nm}, C_{nm}.

Solar radiation pressure. The disturbance due to a solar radiation is given by the formula [2, p. 574]:

$$\vec{a}_{srp} = -\rho_{SR} \frac{c_R A_\odot}{m} \frac{\vec{r}_{sat-Sun}}{|\vec{r}_{sat-Sun}|} \tag{4}$$

where

- ρ_{SR} – is the initial solar radiation, depending on the season and the intensity of solar activity;
- $\rho_{SR} = \frac{P_0}{C}$, where P_0 – is the power of solar radiation acting on 1 cm of the Earth's surface (1358–1373 W/m^2);
- the coefficient of reflectivity C_R determines the reflective and absorbing characteristics of the satellite body material;

Bulletin of L.N. Gumilyov ENU. Mathematics. Computer science. Mechanics series, 2022, Vol. 141, №4

9

- $A_{\odot}$ – the cross-sectional area of the satellite perpendicular to the direction of solar radiation (depends on the mode of operation of the satellite, constantly changes depending on the configuration of the satellite);
- $\vec{r}_{sat-Sun}$ - vector in the direction from the satellite to the Sun;
- m is the satellite's mass.

Lunar-solar disturbances. In the inertial coordinate system associated with the Earth, the acceleration of the satellite caused by the attraction of a body P of point mass M is expressed as follows [7]:

$$\vec{a}_{3Bodies} = \ddot{\vec{r}} - GM \left(\frac{\vec{b} - \vec{r}}{|b - r|^3} - \frac{\vec{b}}{|b|^3} \right) \tag{5}$$

where r and b –are the geocentric coordinates of the satellite and the body P.

To calculate the positions and velocities of the Sun, Moon and major planets, we use high-precision ephemerides $DE440$ and $DE441$ distributed by NASA's JPL Laboratory. These ephemerides are obtained by numerical methods and give coordinates in the form of Chebyshev polynomials in a rectangular barycentric coordinate system with the Earth's equator and equinox, referring to the epoch $J2000$.

Atmospheric Drag. Among the forces of non-gravitational nature, aerodynamic forces acting by the influence of the Earth's atmosphere have the greatest impact on the movement of LEO satellites (i.e. satellites moving at altitudes from 150 to 1500 km). The effect of these forces is mainly expressed in the resistance to the movement of the satellite, directed opposite to its relative velocity [2, p. 551]:

$$\vec{a}_{drag} = \frac{1}{2} \rho \frac{C_D A}{m} v_{rel}^2 \frac{\vec{v}_{rel}}{|\vec{v}_{rel}|} \tag{6}$$

where ρ – the density of the atmosphere, which depends on the selected atmospheric drag model, the composition of the atmosphere, the possibility of propagation, as well as on the solar activity index $F_{10.7}$ and the geomagnetic activity indices K_p, a_p;
C_D – aerodynamic drag coefficient;
$\vec{v}_{rel}$ – relative velocity of the satellite to the rotating atmosphere;
A – area of the satellite.
For the air density function, the approximate expression is valid:

$$\rho = \rho(h) = \rho_0 e^{-h/H},$$

where h is the height at which the density is measured, H is a constant (height scale),
ρ_0- is the density value at the starting point.

The ballistic coefficient $BC = C_D A / 2m$ for the LEO case is usually estimated as part of the extended state vector, since this is one of the main sources of errors.

Time on coordinate systems conversions. Service IERS (International Earth Rotation and Reference Systems Service) is responsible for monitoring the Earth orientation parameters, for maintaining global time and reference frame standards, including time corrections. The Earth Orientation Parameters (EOP) are the parameters provide the rotational part of the transformation between the current releases of the International Terrestrial Reference Frame and the (ITRF) International Celestial Reference Frame (ICRF) as a function of time. In our model, we periodically update information about time corrections and about the Earth's orientation parameters from the IERS bulletins [7]: these are the parameters UT1-TAI, UTC-TAI, GPS-UTC, UT1-UTC [sec]; the coordinates of the pole offset x ["], y["].

2.2 Numerical integration of the ODE describing the satellite's motion.

The efficiency and accuracy of calculations are provided by high-precision numerical methods. As an indicator of the effectiveness of numerical integration methods in propagation the position of the satellite in orbit, it is considered to achieve a given level of accuracy when integrating with

---

[7]International Earth Rotation and Reference Systems Service(IERS Conventions), https://www.iers.org/IERS/EN/Publications/Bulletins/bulletins.html

Л.Н. Гумилев атындағы ЕҰУ Хабаршысы. Математика. Компьютерлік ғылымдар. Механика, 2022, Том 141, №4
Вестник ЕНУ им. Л.Н. Гумилева. Математика. Компьютерные науки. Механика, 2022, Том 141, №4

10

less calculation time, which is equivalent to the number of calls to the right side of the system of ODE(Ordinary differential equations), containing accelerations from all considered disturbing forces acting on the satellite.

To determine the parameters of the satellite motion at time t, it is necessary to solve a system of differential equations (1) with the initial conditions set at time t_0: $(\vec{r}_0, \vec{v}_0)$ $=(x, y, z, v_x, v_y, v_z)|_{t_0}$.

Several types of ODE's numerical integration, describing the motion of the satellite, were considered, including nested Runge-Kutta methods and their modifications. Among the modern methods for solving non-rigid systems of ODE, the best results are obtained by the Dormand-Prince method 8(7) with adaptive step with error control, which was chosen for integrating the system of equations, describing the motion of the satellite(1).

Runge-Kutta methods [8] for solving the differential equation:

$$y' = f(x, y(x)) \tag{7}$$

with an initial condition

$$y(x_0) = y_0 \tag{8}$$

are given by the following calculation formulas of approximate values of the solution $y_{n+1} = y(x_{n+1})$ in the $x_{n+1} = x_n + h_n$:

$$y_{n+1} = y_n + \sum_{i=1}^{s} \alpha_i k_i \tag{9}$$

where

$$k_1 = h_n f(x_n, y_n) \tag{10}$$

$$k_i = h_n f\left(x_n + c_i h_n, y_n + \sum_{j=1}^{i-1} a_{ij} k_j\right), \qquad i = 2, 3, \ldots, s, \tag{11}$$

s – the number of stages of the Runge-Kutta method and

$$c_i = \sum_{j=1}^{i-1} a_{ij}, \qquad\qquad i = 2, 3, \ldots, s. \tag{12}$$

In practice, nested Runge-Kutta formulas are often used, in which, together with formulas (9)-(12), the error estimator formula is used:

$$\hat{y}_{n+1} = y_n + \sum_{i=1}^{s} \widehat{\alpha}_i k_i, \tag{13}$$

where is the new approximate value of $y(x_{n+1})$ calculated with a new set of weight multipliers $\widehat{\alpha}_i$, $i = 1, 2, \ldots, s$.

The approximation orders of the methods given by formulas (9) and (13), as a rule, differ. For such Runge-Kutta methods, the notation RK p(q) is used, where p is the order of approximation of formula (8). q is the order of approximation of formula (13). In [1], Dormand and Prince proposed a modification of the Runge-Kutta method RK8(7) (now designated as DOPRI8(7)). They considered a 13-stage Runge-Kutta method of orders 8(7). To reduce the number of equations, the following additional conditions were proposed (reduced system).

$$\sum_{i=1}^{13} \widehat{\alpha}_i a_{ij} = \widehat{\alpha}_j (1 - c_j), \qquad j = 1, \ldots, 13, \tag{14}$$

$$\sum_{i=1}^{12} \alpha_i a_{ij} = \alpha_j (1 - c_j), \qquad j = 1, \ldots, 12, \tag{15}$$

$$a_{i2} = 0, \qquad i = 4, \ldots, 13, \qquad a_{i3} = 0, \qquad i = 6, \ldots, 13, \tag{16}$$

$$\widehat{\alpha}_i = \alpha_i = 0, \qquad i = 2, \ldots, 5, \tag{17}$$

Bulletin of L.N. Gumilyov ENU. Mathematics. Computer science. Mechanics series, 2022, Vol. 141, №4

11

$$\sum_{j=1}^{12} a_{ij} c_j^k = \frac{c_i^{k+1}}{k+1}, \qquad k = 1, 2;; \quad i = k+2, \ldots, 13, \quad k = 3;; \qquad i = 6, \ldots, 13 \qquad (18)$$

$$\sum_{i=1}^{13} \widehat{\alpha}_i (1 - c_i) a_{ij} = 0, \qquad\qquad j = 4,\ 5, \qquad (19)$$

$$\sum_{i=1}^{13} \widehat{\alpha}_i c_i (1 - c_i) a_{ij} = 0, \qquad\qquad j = 4,\ 5, \qquad (20)$$

$$\sum_{i=1}^{13} \sum_{j=1}^{12} \widehat{\alpha}_i (1 - c_i) a_{ij} a_{jk} = 0, \qquad\qquad k = 4,\ 5, \qquad (21)$$

$$\sum_{i=1}^{13} (\alpha_i - \widehat{\alpha}_i)(1 - c_i) a_{ij} = 0, \qquad\qquad j = 4,\ 5, \qquad (22)$$

This model has 10 free unknowns: c_2, c_3, c_6, c_7, c_8, c_{10}, c_{11}, $\widehat{\alpha}_{13}$, α_{12}, a_{84}. We choose the values of these free unknowns different from each other and at least one of the unknowns $\widehat{\alpha}_{13}$, α_{12} different from zero. The remaining unknowns are found by solving the system (14)-(22). Ratios (14)-(22) for coefficients α_i, $\widehat{\alpha}_i$, $i = 1, \ldots, 13$, c_j, $j = 2, \ldots, 13$, $a_{ij}, j = 1, \ldots, i-1$, $i = 2, \ldots 13$ were proposed in [1]. A set of coefficients satisfying the ratios (14)-(22) were also selected there (see Table 2 in [8]).

The Dormand-Prince method 8(7) has the smallest error among all schemes of the 8th order. Compared with the Fehlberg method, the Dormand-Prince method showed the best results in terms of global error, as well as the total number of calls to the right side of the system with disturbing accelerations acting on the satellite in orbit, as shown in the Table 2.

TABLE 2 – **Global errors of numerical methods for one orbit revolution for the first group of initial values**

Метод	погрешность
Fehlberg45	$7.42775 \cdot 10^{-12}$
DOPRI5	$1.95463 \cdot 10^{-13}$
Fehlberg78	$5.45348 \cdot 10^{-12}$
DOPRI8	$1.06343 \cdot 10^{-13}$

The global error is understood as the maximum value from the norms of the vectors of differences between the exact solution and the numerical solution on the interval grid (the interval is equal to the orbital period, in this case about 97 minutes) using the appropriate integration method in the absence of rounding errors.

$$\varepsilon(\tau) = \max_{1 \le i \le n} |y_i - z_i|,$$

where $|\cdot|$ –is the selected norm in R^m, m is the dimension of the state vector of the satellite, $y_i = \left(x_i^1,\ x_i^2,, x_i^m\right)$ – approximate solution in node t_i; $z_i = z_i(t_i)$ – is the exact solution in the same grid node.

By default, when the state vector consists only of the position vector and the velocity vector of the satellite, then the dimension in the standard case is $m = 6$.

As a rule, numerical integration errors are not a large source of errors compared to errors in modeling the model of perturbing accelerations, which are the main sources of errors. It is assumed that the integration method used is correctly configured with the correct step size control.

2.3 Covariance propagation

In the probabilistic formulation, the position of the satellite in orbit is determined by the results of the propagation of motion parameters and the propagation of the covariance matrix. The probabilistic nature of the satellite's location at the propagated point in orbit is taken into

Л.Н. Гумилев атындағы ЕҰУ Хабаршысы. Математика. Компьютерлік ғылымдар. Механика, 2022, Том 141, №4

Вестник ЕНУ им. Л.Н. Гумилева. Математика. Компьютерные науки. Механика, 2022, Том 141, №4

12

account, based on the accuracy of determining the orbit parameters from GPS navigation data. The accuracy of determining the orbit parameters is set by the covariance matrix at the time of clarifying the initial conditions of the satellite motion.

At the same time, it is assumed that the scattering of the elements of the state vector of the satellite obeys the normal distribution law.

The covariance matrix, in turn determines the scattering ellipsoid (a special case of the phase space region) in which the satellite can be located with a given probability level.
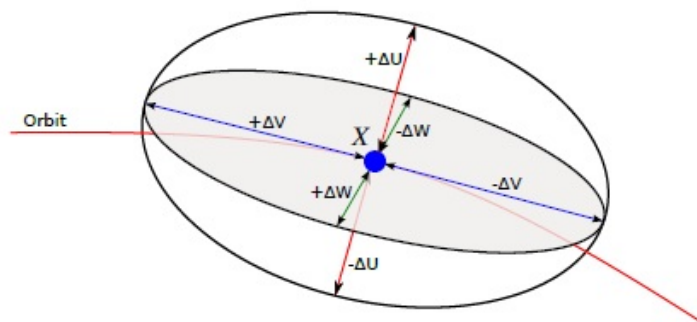
FIGURE 1 – Error ellipsoid

In the probabilistic formulation, an ellipsoid of scattering is defined at any given time, covering a region of space in which a satellite can be located with a given level of probability. Suppose that the scattering cloud is approximated by an ellipsoid of rotation curved along the orbit of the satellite, with axes equal to $\sigma_{\rho\tau n}$. The center of this ellipsoid is the position of the satellite in orbit at the initial epoch.

It is assumed that the measurement errors of the six orbital elements have a normal distribution. Thus, the satellite location error also represents a three-dimensional normal distribution [10], [11]. Covariance matrices should statistically correspond to the actual accuracy of the estimate in accordance with three-dimensional normal (Gaussian) probability distributions.

According to [12], the probability of the distribution of points in an ellipsoid varies as follows:

$$P = \frac{4}{\sqrt{2\pi}} \left(\frac{k^3}{6} - \frac{k^5}{20} + \frac{k^7}{112} - \frac{k^9}{864} + \dots \right),$$

where k-magnification factor.

The probability of the distribution of points in the error ellipsoid changes with the change of K as follows:

at k=1, the probability of distribution of expected data points is 19.9%;

at k=2, the probability of distribution of expected data points is 73.9%;

at k=3, the probability of distribution of expected data points is 97.1%.

The covariance matrix is provided in the form of a symmetric matrix of size 6 x 6 and characterizes the uncertainty in the state vector of the satellite. The diagonal elements represent the variance in each of the components $(R, T, N, \dot{R}, \dot{T}, \dot{N})$, and the non-diagonal terms give the covariance between the two named components. The covariance matrix is represented in the orbital coordinate system (R, T, N, V_R, V_T, V_N):

$$Cov = \begin{pmatrix} CR_R & CT_R & CN_R & C\dot{R}_R & C\dot{T}_R & C\dot{N}_R \\ CR_T & CT_T & CN_T & C\dot{R}_T & C\dot{T}_T & C\dot{N}_T \\ CR_N & CT_N & CN_N & C\dot{R}_N & C\dot{T}_N & C\dot{N}_N \\ CR_{\dot{R}} & CT_{\dot{R}} & CN_{\dot{R}} & C\dot{R}_{\dot{R}} & C\dot{T}_{\dot{R}} & C\dot{N}_{\dot{R}} \\ CR_{\dot{N}} & CT_{\dot{N}} & CN_{\dot{N}} & C\dot{R}_{\dot{N}} & C\dot{T}_{\dot{N}} & C\dot{N}_{\dot{N}} \\ CR_{\dot{T}} & CT_{\dot{T}} & CN_{\dot{T}} & C\dot{R}_{\dot{T}} & C\dot{T}_{\dot{T}} & C\dot{N}_{\dot{T}} \end{pmatrix}$$

Bulletin of L.N. Gumilyov ENU. Mathematics. Computer science. Mechanics series, 2022, Vol. 141, №4

13

This representation allows you to most clearly represent the errors in determining the parameters of the orbit.

A numerical experiment on the propagation of the covariance matrix shows that the diagonal elements of this matrix corresponding to deviations along the radial and normal directions in the orbital coordinate system have a harmonic character.

Let $x(t) = (r_i, r_j, r_k, v_i, v_j, v_k)$ – be the state vector of the satellite. As is known, the state vector can be described by a stochastic dynamical system

$$\dot{x} = f(x, w, t), \tag{23}$$

where w is the noise of the system. Let the measurements z_k of the state vector $x_k = x(t_k)$ at time $t = t_k$ be expressed as follows:

$$z_k = h_k(t_k, \ x_0) + w_k, \tag{24}$$

where w_k – is the noise of the system.

Here h_k denotes the model value of the kth observation as a function of time t_k and the instantaneous state $x(t_0)$ at the initial moment of time. Errors arising from rounding errors, small nonlinearities, simplifying the force model will propagate without further correction by subsequent measurements and will lead to an erroneous and divergent estimation of the satellite state vector. To avoid such a situation, the addition of technological noise (process noise) is used.

The values of w_k take into account the difference between actual and simulated observations due to measurement errors, which are usually considered randomly distributed with a zero mean value.

Let $\hat{x}_{k-1}$ be an estimate of the state vector at time t_{k-1}. Using $\hat{x}_{k-1}$ an a priori estimate of $\hat{x}_k^-$ is obtained. After the measurements z_k a correction of the a priori estimate is carried out and a posteriori estimate of $\hat{x}_k^+$ is obtained.

At the initial moment, the following are given: $\hat{x}_{k-1}, \ \hat{P}_{k-1}$.

The a priori estimate $\hat{x}_k^-$ is obtained by integrating equation (23) with the initial condition on the interval $[t_{k-1}, \ t_k]$ $x(t_{k-1}) = \hat{x}_{k-1}$, i.e.

$$\hat{x}_k^- = \hat{x}_{k-1} + \int_{t_{k-1}}^{t_k} f(\hat{x}_{k-1}, w, t) \, dt. \tag{25}$$

$\dot{\Phi} = \frac{\partial f(x,w,t)}{\partial x} \Phi(t_k, \ t_{k-1})$ with an initial condition $\Phi(t_{k-1}, \ t_{k-1}) = I$.

Errors in modeling the true dynamics of the system at this step may introduce a priori some error in the estimation, which is quantified in the error covariance matrix P_k.

An a priori estimate of the error covariance matrix is obtained from a linearized dynamical system:

$$P_k^- = \Phi_{k-1}(t_k, \ t_{k-1}) P_{k-1}^+ \Phi_{k-1}^T(t_k, \ t_{k-1}) + Q, \tag{26}$$

where

$$\Phi_{k-1} = e^{F_{k-1}\Delta t}, \qquad F_{k-1} = \left. \frac{\partial f(x, w, t)}{\partial x} \right|_{x = \hat{x}_{k-1}}, \tag{27}$$

$$Q = \begin{pmatrix} \sigma_x^2 & 0 & 0 & 0 & 0 & 0 \\ 0 & \sigma_y^2 & 0 & 0 & 0 & 0 \\ 0 & 0 & \sigma_z^2 & 0 & 0 & 0 \\ 0 & 0 & 0 & \sigma_{dx}^2 & 0 & 0 \\ 0 & 0 & 0 & 0 & \sigma_{dy}^2 & 0 \\ 0 & 0 & 0 & 0 & 0 & \sigma_{dz}^2 \end{pmatrix} \tag{28}$$

where Q is the covariance matrix of the system noise.

The expected system noise (system dynamics modeling errors) and measurement noise (irregular measurement fluctuations) are used to weigh the significance of two updates relative to each other.

Л.Н. Гумилев атындағы ЕҰУ Хабаршысы. Математика. Компьютерлік ғылымдар. Механика, 2022, Том 141, №4

Вестник ЕНУ им. Л.Н. Гумилева. Математика. Компьютерные науки. Механика, 2022, Том 141, №4

14

Modeling the noise of the Q process is a difficult task, since it is necessary to take into account various sources of disturbances. These sources are, for example, the geopotential of the Earth, the atmospheric drag/density, the pressure of solar radiation, disturbances from third bodies and tidal forces.

The accuracy of propagation the parameters of the satellite motion is determined by the covariance matrix, which is calculated by the formula (26), with a known matrix at the previous step P_{k-1}^{+}.

$\Phi_{k-1}-$ the matrix of partial derivatives of the elements of the vector of motion parameters at time t by the elements of the vector of motion parameters for the initial epoch. The above ratios (25)-(26) allow us to propagate the covariance matrix together with the parameters of the satellite motion.

Also a method to reduce the influence of numerical errors in calculations for updating the covariance matrix has been applied on propagation process, which together with a highly accurate propagation, can be applied in different satellite's flight control tasks, where the satellite's orbit determination errors taking into account.

3 Results and Discussion

3.1 Developed software «Orbit Propagator tool»

The OPT (Orbit Propagator Tool) software developed by us is based on a high-precision model for orbit propagation of LEO satellites. This software makes it possible, with a given model of satellite motion and known statistical characteristics of orbit determination errors, to propagate the covariance matrix together with the state vector.

The OPT is a software tool designed to support operators in Flight Dynamics routine operations and able to use it for high-precision orbital analysis to support various space missions and planning in-orbit maneuvers. Software tool allows you to propagate the orbital parameters of the satellite (state vector, Keplerian elements) at a given interval with the writing of the results in the selected coordinate system in the report files. Also in the software there is a possibility of constructing two-dimensional graphs of orbital elements for analyzing the evolution of the elements of the satellite orbit.

The software contains a flexible system of configurable parameters of the acceleration model and the integration method (Fig. 2), including the choice of sources of planetary ephemerides, the choice of a set of configuration parameters. And it can be used as a standalone tool or in combination with advanced satellite operations planning tools in orbit. A high level of design flexibility is also achieved due to an extensive set of input and output parameters.

Bulletin of L.N. Gumilyov ENU. Mathematics. Computer science. Mechanics series, 2022, Vol. 141, №4

15

FIGURE 2 − **Configurable parameters of the dynamic model of perturbation forces**

3.2 Simulation data

The results obtained by modeling the satellite motion under various scenarios with a different set of disturbing forces, as well as the use of numerical methods for integrating high orders with automatic step selection, demonstrate high accuracy in propagation the satellite position in orbit. The propagation of the satellite state vector in orbit is based on a dynamic force model that includes the Earth's gravity, polar and ocean tides, lunar-solar disturbances, atmospheric drag and solar radiation pressure, as well as relativistic effects.

On coordinate conversions effect the Parameters of the Earth's rotation of the IAU(The International Astronomical Union) and IERS services are taken into account , as well as the geomagnetic index, atmospheric data from NOAA are taken into account on calculations of acceleration due to atmosphere drag effect.

Several test cases were created for each orbit to test the ability of the OPT software to work accurately using various combinations of forces. The forces used for testing on Earth included models of the Earth's gravitational field $EGM2008$, perturbing accelerations from other planets, modified Harris-Priester models of atmospheric drag and solar radiation pressure (SRP). The degree and order of the geopotential of the Earth were set as constant from $0*20$ to $71*71$. The parameters in Table-4 show the composition and parameters of the disturbing forces used for the test run of the software for demonstration purposes.

All calculations on the numerical integration of the equations of motion of the satellite are carried out in the $ECIJ2000$ coordinate system (an inertial coordinate system with the origin at the center of mass of the Earth for the epoch $J2000$). The duration of the propagation, the size of the report output step and the size of the integrator step varied for different test cases. The time steps of the integrator were chosen for the most accurate comparison of the results of the test case. Units of measurement when comparing state vectors: $m, m/sec$.

For test case, the initial epoch was chosen as 2022/04/28 21:38:30 UTC. The initial conditions used for the test orbits are presented in Tables 3.

When we propagated the orbit of the KazSTSAT satellite, the values of the variables of the perturbing forces model from the following table were used.

Л.Н. Гумилев атындағы ЕҰУ Хабаршысы. Математика. Компьютерлік ғылымдар. Механика, 2022, Том 141, №4

Вестник ЕНУ им. Л.Н. Гумилева. Математика. Компьютерные науки. Механика, 2022, Том 141, №4

16

Table 3 – Initial State vector in Earth Mean Equator and Equinox of J2000 reference frame

	state vector in EME J2000		Kepler elements
x	6652911.169537571	Semi-major axis (a)	6968.860759643917
y	871175.193766317	Eccentricity (e)	0.002351096390
z	1864622.407990260	Inclination (i)	97.621163623454
v_x	2141.603813809	Longitude of the ascending node (Ω)	185.329246514044
v_y	-770.204970971	Argument of perigee (ω)	91.536956373807
v_z	-7217.886453230	Mean anomaly (M)	72.533302431270

Table 4 – Force Model Parameters

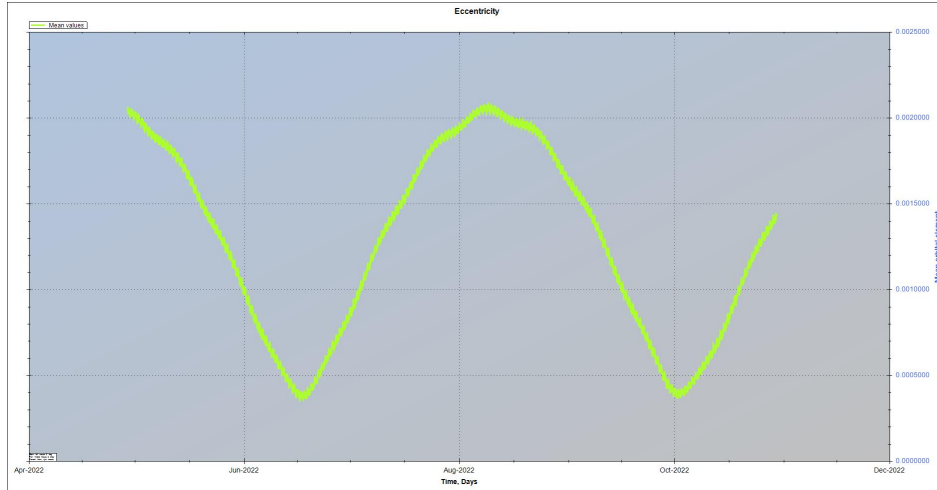| Parameter	OPT
Area[m^2]	0.675
Satellite Mass[kg]	103.9
Integrator	RK7(8)
Integrator error tolerance	1e-013
Integrator error control	Yes
n (degree)	20
m (order)	20
Sun	true
Sun position	True: DE405
Moon	True: DE405
SRad(solar radiation pressure)	True
SRP: sun position	True: DE405
Shadow modeling	Cylindrical
Drag	true
Atmospheric density model	Harris-Priester
Cr(Radiation pressure coefficient)	1.06
Average F10.7	141.5
Atmospheric Drag: Geomagnetic Flux Update	Constant
Geomagnetic index(Kp): JR and MSISE only	3
CD (Drag coefficient)	2.2
ERS EOP format used	Bulletin B(IERS)
Polar Motion calculation	enabled
Solid tides	enabled
Ocean tides	enabled
Relativistic Accelerations	enabled

Table 5 – Parameters and variables of the model of disturbing accelerations

gravity model order	70
mass [kg]	102.89
area [m^2]	0.675
C_r	1.06
C_d	2.2
averageF10_7	141.5
integration step size [s]	10.0
relative error	1E-13
absolute error	1E-09
Sigma	100.0

We took the parameters of the Earth's rotation and time corrections according to the following table.

Bulletin of L.N. Gumilyov ENU. Mathematics. Computer science. Mechanics series, 2022, Vol. 141, №4

17

Table 6 – Earth rotation parameters and time corrections

UT1_UTC	-0.24081
UTC_TAI	-37.0
x_{pole}	0.1627
y_{pole}	0.4322

The results of the OPT propagation are compared with the results obtained in the GMAT(General Mission Analysis Tool) in order to show the equality of the results.

General Mission Analysis Tool (GMAT) is an open source software system for space mission analysis and for solving the navigation tasks developed by NASA in collaboration with Research Institutes.

The GMAT's propagator has been verified and validated [13] against comparison with propagators, that are include as part in Free Flyer and STK. These toolkits are presented as one of the most precise and reliable orbit Simulation tools.

Table 7 – Test scenario: Propagation of the state vector for KazSTSAT satellite on LEO, duration = 1 day. Composition of forces: Earth-EGM96-Sun-Moon- HPAtmModel -SRP- cylindrical

	OPT	GMAT	Differences
x	5152688.373	5152688.531346	0.158346
y	1178317.233	1178317.226069	-0.006931
z	4524117.020	4524116.838835	-0.181165
v_x	5032.404	5032.403807	-0.000193
v_y	-205.331	-205.331045	-0.000045
v_z	-5653.509	-5653.509171	-0.000171

With such a combination of forces, the accuracy of propagation the position of the satellite was 0.240712 meters, according to the velocity vector 0.00026 m/s.

Table 8 – Comparison results after 7 days from the initial epoch. Composition of forces: Earth-EGM96-Sun-Moon-HPAtmModel-SRP- cylindrical State vector in J2000. Epoch 2022/05/05 21:38:30.000 UTC

	OPT	GMAT	Differences
x	-6594221.923000	-6594224.764733	-2.841733
y	-1628674.335000	-1628673.392481	0.942519
z	-1546954.019000	-1546942.627187	11.391813
v_x	-1849.999000	-1849.986891	0.012109
v_y	600.779000	600.781991	0.002991
v_z	7311.571000	7311.573858	0.002858

With such a combination of forces, the accuracy of propagation the position of the satellite was 11.7 meters, with a velocity vector of 0.013 m/s.

It is assumed that the standard deviation of the initial state of the satellite state vector is 100 m (a priori sigma position) and 1 m/s (a priori sigma velocity), respectively. These statistics are used to generate the initial a priori covariance matrix.

When using various combinations of models, we noticed that among the orbital models used for satellite in low-Earth orbit, the geopotential and the atmospheric drag model are the main sources of errors, and therefore they need to be modeled more accurately.

Л.Н. Гумилев атындағы ЕҰУ Хабаршысы. Математика. Компьютерлік ғылымдар. Механика, 2022, Том 141, №4

Вестник ЕНУ им. Л.Н. Гумилева. Математика. Компьютерные науки. Механика, 2022, Том 141, №4

18
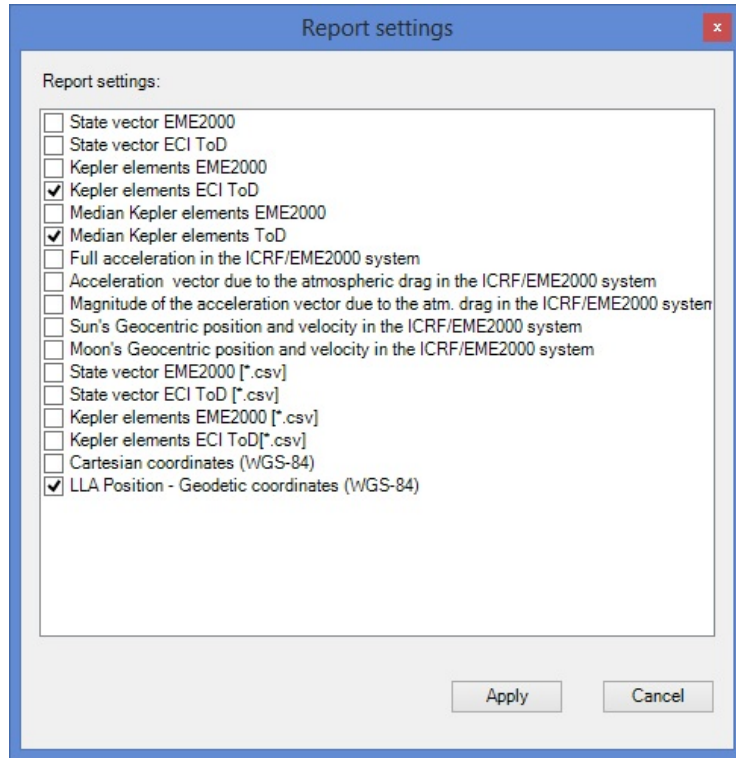
FIGURE 3 – **Composition and form of the output files of the report with ephemerides**

Plot of selected orbital elements in the long-term analysis of the evolution of orbital elements using "medium elements" for a mission in LEO orbit, for example, at an interval of 6 months, are shown in Fig. 6-9.

The computational performance of numerical propagator calculations with a different combination of forces, step and interval is presented in Table-9.

TABLE 9 – **Calculation time for propagation the state vector of the satellite in the OPT software**

Test case	OPT time[sec]
LEO SSO 1 day with step=10 sec: Earth-JGM3(20x20)-Sun-Moon-HPAtmModel - SRP -cylindrical	2.4
LEO SSO 1 day with step=30 sec: Earth-JGM3(20x20)-Sun-Moon-HPAtmModel - SRP -cylindrical	2.0
LEO SSO 3 day with step=10 sec: Earth-JGM3(20x20)-Sun-Moon-HPAtmModel - SRP -cylindrical	6.5
LEO SSO 3 day with step=30 sec: Earth-JGM3(20x20)-Sun-Moon-HPAtmModel - SRP -cylindrical	6.0
LEO SSO 3 day with step=60 sec: Earth-JGM3(20x20)-Sun-Moon-HPAtmModel - SRP -cylindrical	5.9
LEO SSO 7 day with step=10 sec: Earth-JGM3(20x20)-Sun-Moon-HPAtmModel - SRP –cylindrical	15.9
LEO SSO 7 day with step=30 sec: Earth-JGM3(20x20)-Sun-Moon-HPAtmModel - SRP –cylindrical	14.6
LEO SSO 7 day with step=60 sec: Earth-JGM3(20x20)-Sun-Moon-HPAtmModel - SRP -cylindrical	15.1
LEO SSO 7 day with step=300 sec: Earth-JGM3(20x20)-Sun-Moon-HPAtmModel - SRP -cylindrical	13.8
LEO SSO 30 day with step=30 sec: Earth-JGM3(20x20)-Sun-Moon-HPAtmModel - SRP -cylindrical	70.2
LEO SSO 30 day with step=60 sec: Earth-JGM3(20x20)-Sun-Moon-HPAtmModel-SRP -cylindrical	60.3
LEO SSO 30 day with step=300 sec: Earth-JGM3(20x20)-Sun-Moon-HPAtmModel-SRP -cylindrical	61.6
LEO SSO 365.25 days with step=600 sec: Earth-JGM3(20x20)-Sun-Moon-HPAtmModel - SRP -cylindrical	799

Calculations were performed on a portable computer with an Intel Core i7-4710HQ processor with 8 GB RAM.

The presentation of all the results obtained in the software is beyond the scope of one article, so we limited ourselves to demonstrating the operation of the test scenario and the propagation process in the OPT software.

Bulletin of L.N. Gumilyov ENU. Mathematics. Computer science. Mechanics series, 2022, Vol. 141, №4

19
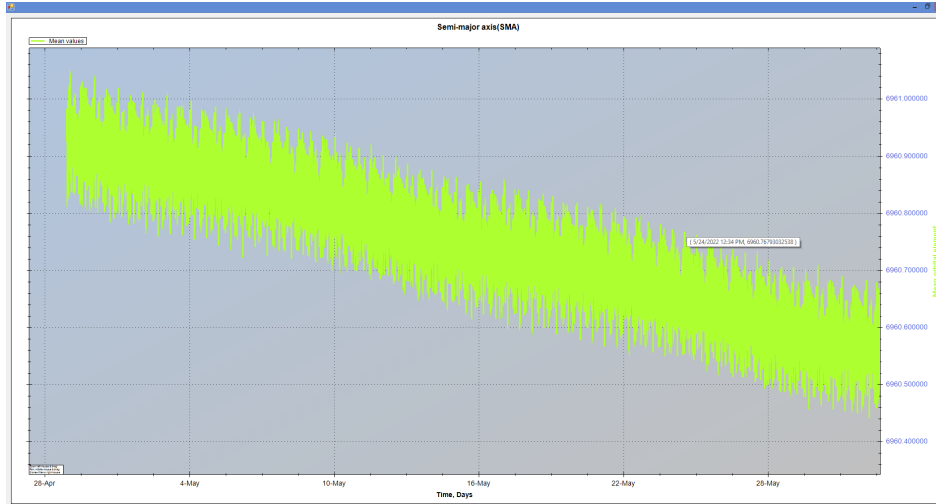
Figure 4 – Evolution of the Semi-major axis in the 30-day interval
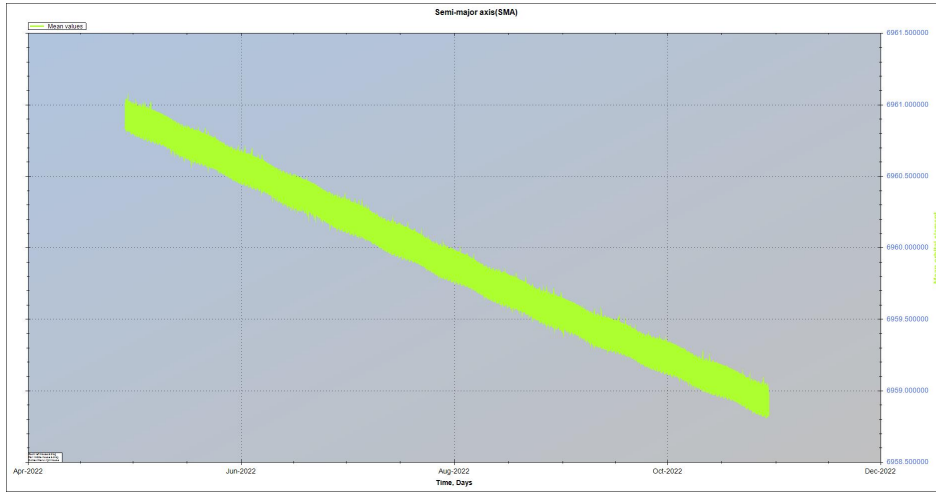
Figure 5 – Evolution of the Semi-major axis over the 6-month interval
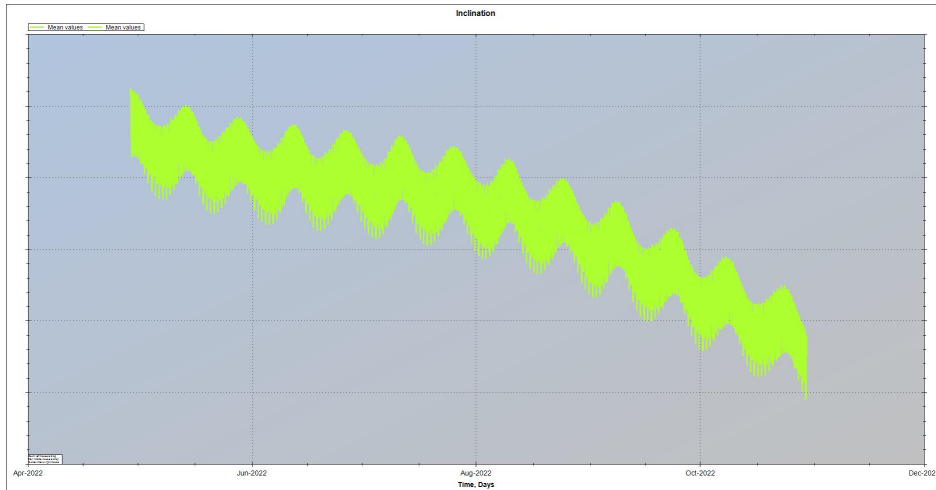
Figure 6 – Evolution of the inclination over the 6-month interval

3.2 Verification

This section describes the validation processes and results for the OPT tool. For a realistic assessment of accuracy, the user must make sure that the models of disturbing forces, respectively, and the propagation results can be trusted with an accuracy above 15 meters.

Л.Н. Гумилев атындағы ЕҰУ Хабаршысы. Математика. Компьютерлік ғылымдар. Механика, 2022, Том 141, №4

Вестник ЕНУ им. Л.Н. Гумилева. Математика. Компьютерные науки. Механика, 2022, Том 141, №4

20

FIGURE 7 − **Evolution of the eccentricity over the 6-month interval**

FIGURE 8 − **Keplerian elements of the orbit in EME J2000**

FIGURE 9 − **Keplerian elements of the spacecraft orbit in the EME ToD (true-of-date epoch)**

Bulletin of L.N. Gumilyov ENU. Mathematics. Computer science. Mechanics series, 2022, Vol. 141, №4

21

FIGURE 10 – The state vector in the EME J2000

The results of the OPT propagation are compared with the results obtained in GMAT[8], as well as with the GPS receiver navigation solution. For example, the residuals resulting on state vectors propagation for 7 days from the same epoch time by both the GMAT and developed OPT tool, are shown in figures 11-12.
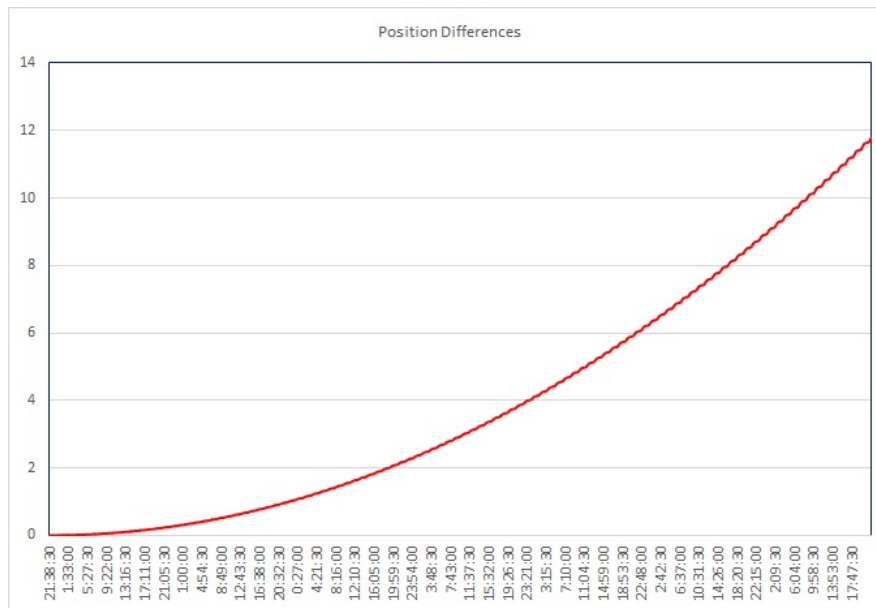
FIGURE 11 – The difference in the position vector over a one-week interval (m)

The OPT propagation results are compared with the GMAT results with the maximum normalized position and velocity difference over the propagation duration. This results displayed in a table format. To determine whether the comparison value of the test case modeled in the software is acceptable, an acceptance matrix was created, presented in Table 10. Comparative results of propagation the satellite orbit on one orbit are shown in tables 11-15, obtained in different coordinate systems.

Also, for verification purposes, we compared the orbit propagation at various time intervals with the navigation solutions of the SGR-07 GPS receiver installed on board the KazSTSAT satellite.

---

[8]General Mission Analysis Tool, Software Package, NASA Goddard Space Flight Center, Greenbelt, MD, 2007, URL: http://gmat.gsfc.nasa.gov

Л.Н. Гумилев атындағы ЕҰУ Хабаршысы. Математика. Компьютерлік ғылымдар. Механика, 2022, Том 141, №4

Вестник ЕНУ им. Л.Н. Гумилева. Математика. Компьютерные науки. Механика, 2022, Том 141, №4

22
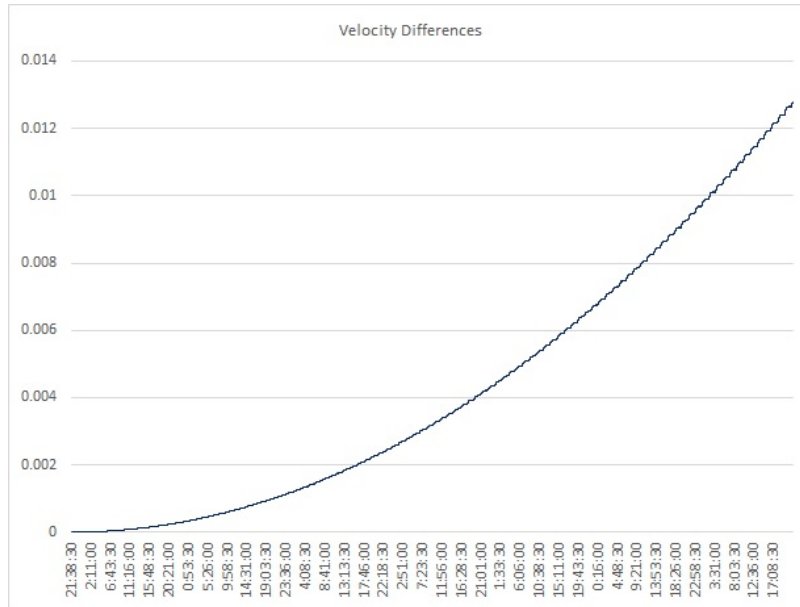
FIGURE 12 − **The difference in the velocity vector over a one-week interval (m/s)**

TABLE 10 − **Acceptance Matrix**

Difference in	Acceptable position difference (m)
Non-spherical gravity	<0.001
Point mass gravity	<0.001
Solar radiation Pressure	<0.6
Atmospheric Drag	<20

TABLE 11 − **The test scenario for comparing of the OPT/GMAT software results (Sun-synchronous orbit)**

Test case	Position difference(m)	Velocity difference(m/s)
Earth-JGM3-0-0-0-0	1.203	0.002
Earth-JGM3-Sun-0-0-0	1.203	0.001
Earth-JGM3-Sun-Moon-0-0	1.203	0.002
Earth-JGM3-Sun-Moon-0-SRP-cylindrical	1.020	0.001
Earth-JGM3-Sun-Moon-HPAtmModel-0	1.281	0.0015
Earth-JGM3-Sun-Moon-HPAtmModel-SRP	1.2	0.001
Earth-JGM3-Sun-Moon-HPAtmModel-SRP-cylindrical	1.0402	0.0009

TABLE 12 − **The test scenario for comparing of the OPT/GMAT software results (Sun-synchronous orbit)**

Test case	State vector (OPT) (m, m/s)	State vector (GMAT) (m, m/s)	delta
Earth-JGM3-Sun-Moon-HPAtmModel-SRP-cylindrical	-1344.43852	-1344.438283	-0.23726362
	4977.977623	4977.979675	-2.052247331
	-4697.661829	-4697.659723	-2.10593889
	0.0492403	0.049241026	0.0007259
	5.181641	5.181639	-0.0020000
	5.4932774	5.493279382	0.001981803

Bulletin of L.N. Gumilyov ENU. Mathematics. Computer science. Mechanics series, 2022, Vol. 141, №4

23

TABLE 13 – The test scenario: KazSTSAT, 2019/01/17 12:00:00.0 UTC (EME J2000)

	X(m)	Y(m)	Z(m)	Vx(m/s)	Vy(m/s)	Vz(m/s)
OPT	241433.619705	6487906.368239	2536797.612833	1009.703000	2747.069500	6970.948231
GMAT	241433.619705	6487906.368239	2536797.612833	1009.703000	2747.069500	6970.948231
delta	0	0	0	0	0	0

TABLE 14 – The state vector in the EME True-of-Date coordinate system

	X(m)	Y(m)	Z(m)	Vx(m/s)	Vy(m/s)	Vz(m/s)
OPT	-209600.1997021	-6488907.1731688	-2537067.7599385	-1008.5101100	2742.6862989	-6972.8465815
GMAT	-209600.199642	-6488907.1731640	-2537067.759955	-1008.5101100	2742.6862990	-6972.8465820
delta	5.92E-05	4.8E-06	-1.7E-05	0	1E-07	-5E-07

TABLE 15 – Keplerian elements of the orbit in EME J2000

	X(m)	Y(m)	Z(m)	Vx(m/s)	Vy(m/s)	Vz(m/s)
OPT	6967400.359	0.002037	97.868045	90.96413	99.216281	102.110747
GMAT	6967400.359	0.002037	97.868045	90.96413	99.216281	102.110747
delta	-3.99537E-07	0	0	0	0	0

SGR-07 receives and decodes L-band signals from four or more GPS satellites and, using range determination methods, is able to calculate the location of the satellite with an accuracy of 15-25 meters, as well as determine the exact speed and time.

The SGR-07 receiver tracks C/A code signals at the L1 frequency from GPS satellites. Each channel performs measurements of pseudorange, Doppler frequency shift and carrier phase in the measurement epoch. These "raw" measurements are used to calculate the receiver position, velocity and time (Position/Velocity/Time). The position and velocity are transmitted as arrays of vectors in the WGS-84 coordinate system with reference to UTC time. The time is represented as an exact location timestamp sent in GPS time format: the number of the week, the number of seconds from the beginning of the current week and a fraction of a second.

Many tests were performed with a full set of considered disturbing accelerations. In OPT software, when propagation movement, one of the processed vectors from a set of navigation solutions that has been preprocessed was selected as initial conditions. During preprocessing, abnormal errors were discarded according to the $3 \cdot \sigma$ rule. Intervals were selected for propagation the position of the satellite representing the passive sections of the satellite flight: 1 day, 3 days, 7 days, 14 days and 30 days. Then the propagated state vectors of the satellite at the end of the interval in the EME J000 coordinate system were compared with the vector obtained by the GPS navigation solution at the end of the considered intervals.

TABLE 16 – The state vector refined by GPS data and the corresponding orbital elements(true-of-date)

epoch	2022/04/28 21:38:38.000 UTC		
Keplerian elements (ToD)	value	State vector(ToD)	value
Semi-major axis (a)	6960.925018138310	r_x	6623658.751
Eccentricity (e)	0.002047257271	r_y	903162.936
Inclination (i)	97.635627176777°	r_z	1950898.625
Longitude of the ascending node (Ω)	185.592351005803°	v_x	2238.240858
Argument of perigee (ω)	85.199606512757°	v_y	-751.488029
Mean anomaly (M)	78.777122748204°	v_z	-7190.619141

Given the accuracy of determining the GPS receiver, it can be argued that the accuracy of orbit propagation allows using this model and the integration method to solve most problems of satellite orbit control.

Л.Н. Гумилев атындағы ЕҰУ Хабаршысы. Математика. Компьютерлік ғылымдар. Механика, 2022, Том 141, №4

Вестник ЕНУ им. Л.Н. Гумилева. Математика. Компьютерные науки. Механика, 2022, Том 141, №4

24

TABLE 17 – **Comparison of the satellite orbit propagation at the end of the one-week interval with the orbit from the GPS receiver navigation solution**

epoch	2022/05/05 21:38:38.000 UTC		
Keplerian elements (ToD)	OPT	GPS	difference
Semi-major axis (a)	6969.242572	6969.242560	-1.2986E-05
Eccentricity (e)	0.001758	0.001759	-1.72E-07
Inclination (i)	97.628551°	97.628552	-2.13E-07
Longitude of the ascending node (Ω)	192.397495°	192.397494	-1.634E-06
Argument of perigee (ω)	63.393216°	63.393216	-1.94E-07
Mean anomaly (M)	283.824257°	283.824255	-2.405E-06

4 Conclusion

In this research integration methods and a model of disturbing accelerations acting on the satellite were studied. The efficiency of using the modified Dormand-Prince method 8(7) with adaptive step with error control for the numerical solution of differential equations describing the motion of the spacecraft to achieve a high accuracy during orbit propagation is shown.

The main purpose of this work was to show that the used propagation model and the integration method provide sufficient accuracy and are suitable for propagation the position of the satellite, both on short-term and long-term time intervals. The use of an accurate model of disturbing accelerations, using numerical methods of integration of high orders with automatic step selection, demonstrated high accuracy of refinement of the state vector of the satellite in orbit. It also provides a better estimate of the speed and, consequently, a better accuracy of the propagation, thereby improving the accuracy in secondary tasks of satellite orbit control and the accuracy of planning operations with the satellite payload.

The high-precision orbit propagation together with the updating the covariance matrix, can be applied in many actual tasks on Flight Control Operational Planning and the safety in orbit, where the orbit determination errors taking into account.

Such an approach, for example, has found its application for the task of Conjunction Assessment analysis for closest approach cases between two space objects, where the collision avoidance maneuver decision making process is based on a probabilistic approach.

The developed OPT software can be used as the basis for a number of applied tasks for ballistic support the flight control of the satellite's missions on LEO.

References

1 Prince P.J., Dormand J.R., High order embedded Runge-Kutta formulae// Journal of Computational and Applied Mathematics. -1981. -Vol. 7(1). -P. 67-75.

2 Vallado D. A., Fundamentals of Astrodynamics and Applications. - 4th Ed. -2013. -1106 p.

3 Capderou M.,Satellites Orbits and Missions, Springer-Verlag France. 2005. p. 67.

4 Pavlis N.K., Holmes S.A., Kenyon S.C., Factor J.K. An Earth Gravitational Model to Degree 2160: EGM2008; presented at the 2008 General Assembly of the European Geosciences Union, Vienna, Austria, 2008, April 13-18.

5 Rizos C., Stolz A. Force modelling for GPS satellite orbits, Proceedings of the 1st International Symposium Precise Positioning with GPS. -1985. -Vol. 1. P. 87–98.

6 Love A.E.H. The yielding of the earth to disturbing forces. Proceedings of the Royal Society A. -1909. -Vol. 82. №551.

7 Escobal, Pedro R., Methods of Orbit Determination. New York: John Wiley & Sons. (Reprint edition. Malabar FL: Krieger Publishing Co.), 1965, p. 37

8 Hairer E., Norsett S.P., Wanner G., Solving Ordinary Differential Equations I. Nonstiff Problems. Springer Series in Computational Mathematics. Springer-Verlag Berlin Heidelberg, 1993.

9 Wang H.B., Xue F., and Liu C.J. Test method of satellite coverage area and its engineering application//Radio Communications Technology. -2010. -Vol. 3. -P. 19.

10 Wang M., Ma L., Zhang L., and Ji H. Analysis of horizontal positioning error distribution of the Chinese area positioning system// Astronomical Research & Technology. -2012. -Vol. 9. №3. -P. 522-526.

11 Dai G., Chen X., Zuo M., Peng L., Wang M. and Song Z. The Influence of Orbital Element Error on Satellite Coverage Calculation//International Journal of Aerospace Engineering. -2018. -Vol. 2018. -P. 6.

Bulletin of L.N. Gumilyov ENU. Mathematics. Computer science. Mechanics series, 2022, Vol. 141, №4

25

12 Vallado D.A., An analysis of state vector propagation using differing flight dynamics programms. Paper AAS 05-199 presented at the AAS/AIAA Space Flight Mechanics Conference. Copper Mountaun, CO, 2005.

13 Hughes SP, Qureshi RH, Cooley DS, Parker JJ, Grubb TG, Verification and validation of the general mission analysis tool (GMAT), in 2014 AIAA/AAS Astrodynamics Specialist Conference, San Diego, CA, 4-7 Aug 2014.

А.Г. Есенғалиев [1] , **А.Б. Муканов** [2]

[1] *«Ghalam» ЖШС, Тұран даңғ., 89, Астана, Қазақстан*

[2] *М.В.Ломоносов атындағы Мәскеу Мемлекеттік Университетінің Қазақстан Филиалы, Қажымұқан көш., 11, Астана, Қазақстан*

Ковариациялық матрица болжамымен жоғары дәлдіктегі қозғалыс болжамы

Аннотация. Бұл мақалада Ғарыш Аппараттардың(ҒА) позициясын жоғары дәлдікпен болжау моделін қолдану ұсынылады, онда бұзылған үдеулер анықталады, сонымен қатар алынған сандық нәтижелер ұсынылады. Ғарыш Аппараттарына әсер ететін барлық бұзушы күштер модельденеді, атмосфералық қарсылық моделінің параметрлерінің, сондай-ақ IERS, EOP параметрлерінің өзекті деректері қолданылады. LEO-дағы орбиталық позицияны болжауға арналған әзірленген бағдарламалық қамтамасыз ету ҒА ұшуын басқаруды қолдау үшін қолданылады, бұл ретте апталық уақыт аралығындағы ҒА позиция векторы бойынша 10-15 метр деңгейдің дәлдігі қамтамасыз етіледі. ҒА қозғалысының берілген моделінде және күй векторымен бірге орбитаны анықтау қателіктерінің белгілі статистикалық сипаттамаларында ковариациялық матрица болжанады, бұл белсенді ҒА орбитасын басқарудың көптеген өзекті мәселелерінде қолданылады.

Түйін сөздер: ғарыш кемесі; ҒА позициясын болжау; орбитаны анықтау; төмен орбиталық орбита; орбитаны бағалау; бұзушы күштер; сандық интеграция; Рунге-Кутта әдістері, ковариациялық матрица.

А.Г. Есенғалиев [1] , **А.Б. Муканов** [2]

[1] *Ghalam LLP, пр. Туран, 89, Астана, Казахстан*

[2] *Казахстанский филиал МГУ им. М.В. Ломоносова, ул. Кажымукана 11, Астана, Казахстан*

Высокоточный прогноз движения КА с прогнозом ковариационной матрицы

Аннотация. В данной статье предлагается использовать модель высокоточного прогнозировании положения КА, в которой возмущающие ускорения определены, а также представлены полученные численные результаты.

Все возмущающие силы, действующие на Космический аппарат(КА) моделируются, используются актуальные данные параметров модели атмосферного сопротивления, и также параметров IERS, EOP. Разработанное Программное обеспечение (ПО) для прогнозирования положения КА по орбите на LEO применимо для поддержки управления полетом КА, при этом обеспечивается точность уровня в 10-15 метров по вектору положения КА на недельном интервале времени.

При заданной модели движения КА и известных статистических характеристиках погрешностей определения орбиты вместе с вектором состояния прогнозируется и ковариационная матрица, что нашло применение во многих актуальных задачах по поддержке Динамики полета КА.

Ключевые слова: Космический Аппарат, прогнозирование положения КА, определение орбиты, низкоорбитальная орбита, оценка орбиты, возмущающие силы, численное интегрирование, методы Рунге-Кутта, ковариационная матрица.

References

1 Prince P.J., Dormand J.R., High order embedded Runge-Kutta formulae, Journal of Computational and Applied Mathematics. 1981. Vol. 7(1). P. 67-75.

2 Vallado D. A., Fundamentals of Astrodynamics and Applications. 4th Ed. 2013. 1106 p.

3 Capderou M. Satellites Orbits and Missions, Springer-Verlag France. 2005. 67 p.

4 Pavlis N.K., Holmes S.A., Kenyon S.C., Factor J.K. An Earth Gravitational Model to Degree 2160: EGM2008; presented at the 2008 General Assembly of the European Geosciences Union, Vienna, Austria, 2008, April 13-18.

5 Rizos C., Stolz A. Force modelling for GPS satellite orbits, Proceedings of the 1st International Symposium Precise Positioning with GPS. 1985. Vol. 1. P. 87-98.

6 Love A.E.H. The yielding of the earth to disturbing forces. Proceedings of the Royal Society A. 1909. Vol. 82. №551.

7 Escobal, Pedro R., Methods of Orbit Determination. New York: John Wiley & Sons. (Reprint edition. Malabar FL: Krieger Publishing Co.), 1965, p. 37

8 Hairer E., Norsett S.P., Wanner G., Solving Ordinary Differential Equations I. Nonstiff Problems. Springer Series in Computational Mathematics. Springer-Verlag Berlin Heidelberg, 1993.

9 Wang H.B., Xue F., and Liu C.J. Test method of satellite coverage area and its engineering application, Radio Communications Technology. 2010. Vol. 3. P. 19.

10 Wang M., Ma L., Zhang L., and Ji H. Analysis of horizontal positioning error distribution of the Chinese area positioning system, Astronomical Research & Technology. 2012. Vol. 9. №3. P. 522-526.

11 Dai G., Chen X., Zuo M., Peng L., Wang M. and Song Z. The Influence of Orbital Element Error on Satellite Coverage Calculation, International Journal of Aerospace Engineering. 2018. Vol. 2018. P. 6.

12 Vallado D.A., An analysis of state vector propagation using differing flight dynamics programms. Paper AAS 05-199 presented at the AAS/AIAA Space Flight Mechanics Conference. Copper Mountaun, CO, 2005.

13 Hughes SP, Qureshi RH, Cooley DS, Parker JJ, Grubb TG, Verification and validation of the general mission analysis tool (GMAT), in 2014 AIAA/AAS Astrodynamics Specialist Conference, San Diego, CA, 4-7 Aug 2014.

Information about authors:

Есенгалиев Арман Гибатович – **Байланыс үшін автор,** Ғарыштық Технологияның Арнайы Конструкторлық-технологиялық бюросы(ҒТ АКТБ) жетекші инженер-конструкторы, "Ghalam" LLP, Туран даңг., 89, Астана, Казақстан.

Муканов Асхат Бирлесович – PhD, аға оқытушы, М.В. Ломоносов атындағы Мәскеу мемлекеттік университетінің Қазақстан филиалы, Кажымұқан көш., 11, Астана, Казақстан.

Yessengaliyev Arman – **Corresponding author,** Lead design engineer of the Special Design and Technology department, Ghalam LLP, 89, Turan avenue, Astana, Kazakhstan.

Mukanov Askhat – PhD in Mathematics, Senior Lecturer, Kazakhstan Branch of Lomonosov Moscow State University, Kazhymukan str. 11, Astana, Kazakhstan.

Bulletin of L.N. Gumilyov ENU. Mathematics. Computer science. Mechanics series, 2022, Vol. 141, №4

27